

Interpretation of topologically restricted measurements in lattice σ -models

Irais Bautista^a, Wolfgang Bietenholz^a, Urs Gerber^a,
Christoph P. Hofmann^b, Héctor Mejía-Díaz^a and Lilian Prado^a

^a Instituto de Ciencias Nucleares, Universidad Nacional Autónoma de México
A.P. 70-543, C.P. 04510 México, Distrito Federal, Mexico

^b Facultad de Ciencias, Universidad de Colima
Bernal Díaz del Castillo 340, Colima C.P. 28045, Mexico

E-mail: wolbi@nucleares.unam.mx

Abstract. We consider models with topological sectors, and difficulties with their Monte Carlo simulation. In particular we are concerned with the situation where a simulation has an extremely long auto-correlation time with respect to the topological charge. Then reliable numerical measurements are possible only within single topological sectors. The challenge is to assemble such restricted measurements to obtain an approximation for the full-fledged result, which corresponds to the correct sampling over the entire set of configurations. Under certain conditions this is possible, and it provides in addition an estimate for the topological susceptibility χ_t . Moreover, the evaluation of χ_t might be feasible even from data in just one topological sector, based on the correlation of the topological charge density. Here we present numerical test results for these techniques in the framework of non-linear σ -models.

1. Topological sectors in quantum physics

We are going to consider quantum physics in the functional integral formulation with Euclidean time. For a number of models, the paths — or configurations — to be summed over split into *topological sectors*. The simplest example is the quantum rotor, *i.e.* a quantum mechanical scalar particle moving freely on a circle with periodic boundary conditions in time (say with period T). This corresponds to the 1d $O(2)$ model with the action, partition function and expectation values

$$S[\varphi] = \frac{\beta}{2} \int_0^T \dot{\varphi}^2 dt, \quad Z = \int D\varphi \exp(-S[\varphi]), \quad \langle \mathcal{O} \rangle = \frac{1}{Z} \int D\varphi \mathcal{O}[\varphi] \exp(-S[\varphi]). \quad (1.1)$$

(β represents the inverse coupling for the $O(2)$ model, or the moment of inertia for the rotor.) The functional integral $\int D\varphi$ sums over all closed paths $\varphi(t) \in S^1$, $\varphi(0) = \varphi(T)$. These paths occur in disjoint subsets, which can be labelled by their winding number, or *topological charge*

$$Q = \frac{1}{2\pi} \int_0^T \dot{\varphi} dt \in \mathbb{Z}. \quad (1.2)$$

A continuous deformation of a path does not change Q , hence it remains in the same subset, *i.e.* in the same topological sector.

This can be generalised to quantum field theory on a torus, namely to $O(N)$ models in $d = N - 1$ dimensions, where the field is a classical spin $\vec{S}(x) \in S^{N-1}$. For the models in this class, the configurations are structured in topological sectors. We are going to address the cases $N = 2$ and 3 . Further models with topological sectors are *e.g.* the 2d $CP(N - 1)$ models, 2d $U(1)$ gauge theory, and 4d Yang-Mills theories. In all these cases, the configurations can only be deformed continuously within a fixed topological sector. The functional integral splits into disjoint integrals over these sectors, which are characterised by a topological charge $Q \in \mathbb{Z}$.

2. Lattice regularisation and Monte Carlo simulation

We proceed to the lattice formulation, which reduces the (periodic) volume to a set of discrete sites x , say with a cubic structure and lattice spacing a . Matter fields live on these sites, Φ_x , while gauge fields can be given by compact link variables $U_{x,\mu} \in \{\text{gauge group}\}$, $\mu = 1 \dots d$. This represents a gauge invariant UV regularisation.

On the lattice regularised level, there are *a priori* no topological sectors; all configurations can be continuously deformed into one another. Still, something similar exists: the action may have local minima, and their vicinities are separated by regions of high action. Hence transitions between these sectors are statistically suppressed, where

$$p[\Phi] = \exp(-S[\Phi])/Z \tag{2.1}$$

is interpreted as the probability for some configuration $[\Phi]$. In such cases, it is often convenient to introduce a topological charge Q even on the lattice. In the presence of chiral fermions (with a lattice Dirac operator that obeys the Ginsparg-Wilson Relation), this can be done best by the fermion index [1]. For $(N - 1)$ -dimensional $O(N)$ models, the optimal formulation maps local patches of the lattice configuration onto S^{N-1} , and the (hyper-)spherical area represents the topological charge density (“geometric definition”) [2]. These definitions both have the virtue that they provide integer Q values for each configuration (up to a subset of measure zero), even on the lattice.

Monte Carlo simulations generate a sequence of configurations (a “Monte Carlo history”) randomly with the probability given in eq. (2.1). Summing over this set provides an approximation for expectation values of observables, such as n -point functions. There are still statistical errors (the set of configurations is finite), and systematic errors (for instance due to the finite lattice spacing $a > 0$), which can be reduced with increased computational effort. On the other hand, we stress that this method is fully *non-perturbative*.

3. Topologically frozen numerical measurements

Most popular algorithms generate configurations by performing a long sequence of local updates, until a new, (quasi-)independent configuration emerges, to be used for the numerical measurement. This includes in particular the Hybrid Monte Carlo (HMC) algorithm [3], which is standard in QCD simulations with dynamical quarks.

Regarding theories with topological sectors, however, such local update algorithms are plagued by the problem that they have a hard time to change the topological sector. This requires the sequence of update steps to pass through a region of low probability. However, in order to sample the entire space of configuration correctly, the algorithm is supposed to change Q frequently. As a striking counter-example, we mention the QCD study with chiral quarks reported in Ref. [4], where the extensive HMC history was entirely confined to the sector with $Q = 0$. For Wilson-type quarks the problem is less severe so far, *i.e.* in the range of lattice spacings $0.05 \text{ fm} \lesssim a \lesssim 0.15 \text{ fm}$ which have typically been used up to now. However, once we push for even finer lattices — in order to suppress further the systematic lattice artifacts — the problem will become more severe: it is welcome for many reasons that the system is more continuum-like, but this also makes topological transitions harder.

Therefore Monte Carlo histories which are trapped in one topological sector for a very long (computing) time, *i.e.* over a huge number of update steps, are a serious issue. The question arises if we can still perform correct numerical measurements of n -point functions, or *e.g.* of the topological susceptibility

$$\chi_t = (\langle Q^2 \rangle - \langle Q \rangle^2) / V . \quad (3.1)$$

As a remedy, the use of open boundary conditions has been advocated [5]; then Q is not integer anymore, so it can vary continuously. Here we consider attempts to deal with this problem while keeping the boundary conditions periodic. We test two procedures for this purpose, with numerical data for the 1d $O(2)$ and the 2d $O(3)$ model, and we refer to the geometric definition of the topological charge of a lattice configuration. Its contributions from some local patches (nearest neighbour sites in $d = 1$, triangles in $d = 2$) are the lattice topological charge density q .

4. Correlation of the topological charge density

First we consider a method suggested in Ref. [6] to determine χ_t even if only one single topological sector has been explored in the simulation. We denote the restricted expectation value within one sector as $\langle \dots \rangle_Q$. Ref. [6] derived an approximate formula for the correlation of the topological lattice charge density at large Euclidean time separation t ,¹

$$\lim_{t \rightarrow \infty} \langle q_0 q_t \rangle_{|Q|} \approx -\frac{1}{V} \chi_t + \frac{Q^2}{V^2} . \quad (4.1)$$

The derivation assumes the charges Q to be Gauss distributed around zero, $\langle Q^2 \rangle = V \chi_t$ to be large, and $|Q| / \langle Q^2 \rangle$ to be small. The explicit meaning of these requirements remains to be investigated numerically.² Here we give preliminary results of our ongoing study [9]. For the 1d $O(2)$ model we consider the standard lattice action (we will call it simply “standard action”) and the Manton action [10]. For the sum over all topological sectors, analytical results are given in Ref. [11], and additional numerical results in Ref. [12]. For the 2d $O(3)$ model we simulated the standard action (in lattice units)

$$S[\vec{S}] = \beta \sum_{x,\mu} (1 - \vec{S}_x \cdot \vec{S}_{x+\hat{\mu}}) , \quad (4.2)$$

where $\hat{\mu}$ is a lattice unit vector in μ -direction.³ We used an efficient cluster algorithm [13], which is not restricted to local update steps, and which does therefore change the topological sector frequently. Hence in these tests correctly distributed configurations are available, and they provide a check for the indirect methods. The latter are relevant for instance in gauge theories, where no efficient cluster algorithm is known.

Our results for $\langle q_0 q_t \rangle_{|Q|}$ are shown in Figures 1 and 2. In all cases we observe excellent agreement with the values corresponding to the approximation formula (4.1). However, in the field theoretic example of Figure 2 the correlation length is short ($\xi \simeq 1.3$). To move closer to the continuum limit, we have to increase β , and — in order to keep $\langle Q^2 \rangle$ relatively large — also the volume V . Consequently the predicted plateaux for $\langle q_0 q_t \rangle_{|Q|=0,1,2}$ move rapidly towards zero, and it will be difficult to disentangle them in the numerical data from each other and from zero. However, this distinction is crucial for the evaluation of χ_t . The question how far this is still feasible is currently under investigation. Of course, this issue is even more severe in higher dimensions.

¹ On the right-hand-side there is another correction term, $(\langle Q^4 \rangle - 3\langle Q^2 \rangle^2) / (2V \chi_t^2)$, for deviations from Gauss-distributed charges Q (“kurtosis”), but we checked that it is negligible in the examples that we considered.

² Actually there is already a successful determination of χ_t in 2-flavour QCD along these lines [7], but it used the flavour singlet pseudo-scalar density, as suggested in Ref. [8].

³ The Manton action replaces the function $\cos \Delta\varphi_{x,\mu}$ of the relative angle (in the last term) by $\frac{1}{2}(\Delta\varphi_{x,\mu})^2$. For the quantum rotor this reduces the lattice artifacts drastically; this action turns out to be classically perfect [11].

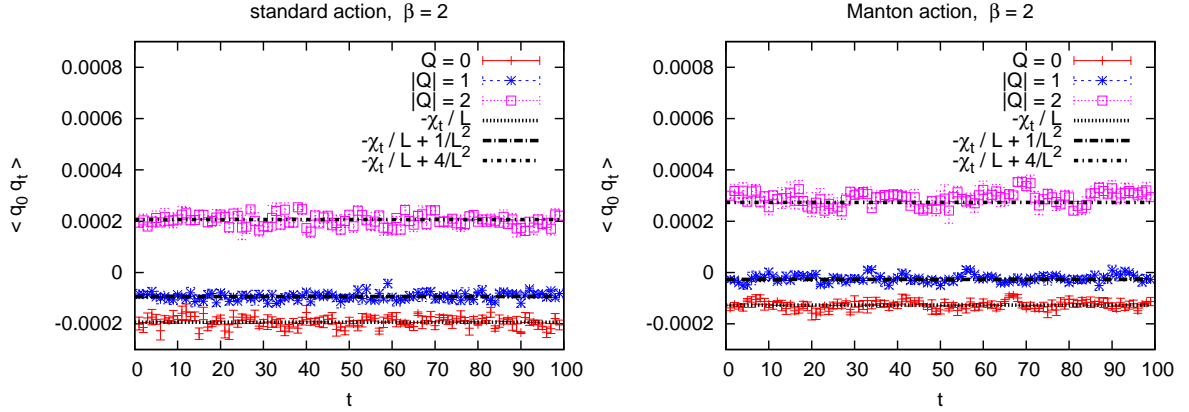


Figure 1. The correlation function of the topological charge density over Euclidean time separation t for the 1d $O(2)$ model on a spin chain of length $L = 100$ and inverse coupling $\beta = 2$. We show results for the standard action (with $\langle Q^2 \rangle = 1.94$) on the left, and for the Manton action (with $\langle Q^2 \rangle = 1.27$) on the right. The black dotted lines correspond to the approximation (4.1) for $|Q| = 0, 1, 2$, if we insert the analytically known values for χ_t [11].

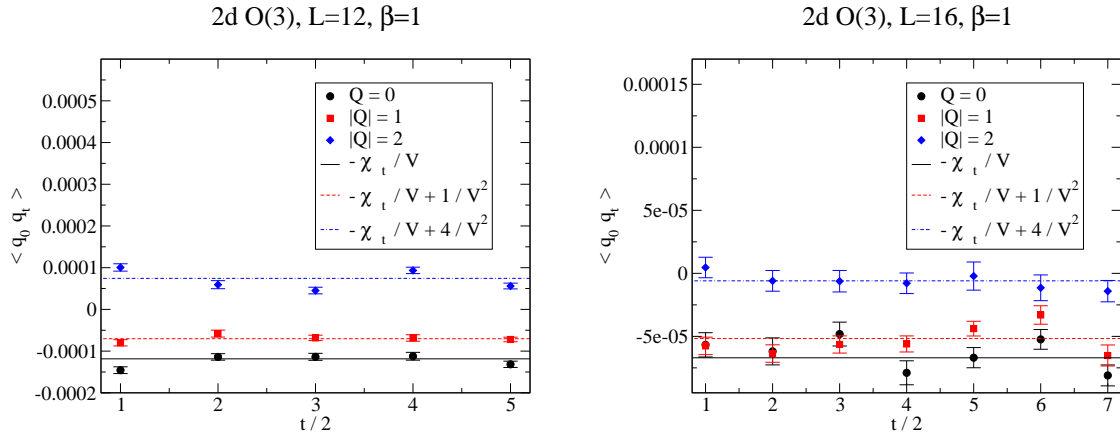


Figure 2. The correlation function of the topological charge density over Euclidean time separation t for the 2d $O(3)$ model at $\beta = 1$. We show results for the standard action in volume $V = 12 \times 12$ (with $\langle Q^2 \rangle = 2.46$) on the left, and $V = 16 \times 16$ (with $\langle Q^2 \rangle = 4.39$) on the right. The horizontal lines are the values for $|Q| = 0, 1$ and 2 obtained from the approximation (4.1), if we insert the directly measured topological susceptibility χ_t .

5. Approximate topological summation of observables

Now we proceed to a more ambitious goal: the computation of some observable $\langle \mathcal{O} \rangle$, if only a few topologically restricted measurements $\langle \mathcal{O} \rangle_{|Q|}$ are available. An approximate formula for this purpose was first derived in Ref. [14], referring to the pion mass in QCD simulations (for later considerations, see Refs. [6, 15–17]). It can also be applied to other observables \mathcal{O} , and other models with topological sectors. The relevant approximation formula reads

$$\langle \mathcal{O} \rangle_{|Q|} \approx \langle \mathcal{O} \rangle + \frac{c}{2V\chi_t} \left(1 - \frac{Q^2}{V\chi_t} \right), \quad (5.1)$$

where c is a constant, which (like χ_t and $\langle \mathcal{O} \rangle$) stabilises in large volumes. Together with $\langle \mathcal{O} \rangle$ and χ_t , there are three unknown terms on the right-hand-side. If we employ numerical results for the left-hand-side, in various $|Q|$ and V , they can in principle be determined by a fit (this requires results in at least two different volumes).

The assumptions in the derivation are (qualitatively) the same as for eq. (4.1), hence we need again a reasonably large $\langle Q^2 \rangle = V\chi_t$, and we should only use rather small charges $|Q|$. Up to now there are only few tests of this approximation with numerical data; they were performed in the Schwinger model [15, 17] and for the quantum rotor [16].

First we present further results for the latter, *i.e.* the 1d $O(2)$ model, where we measured the restricted correlation length $\xi_{|Q|}$ for $|Q| = 0, 1, 2$. Actually the (connected) correlation function exhibits a neat exponential decay — resp. a cosh shape — only if all sectors are included. Topological restriction deforms this decay somewhat, hence the evaluation of $\xi_{|Q|}$ is less obvious [16, 17]. To illustrate this property, we show in Figure 3 the correlation function in a small volume of $L = 14$ at $\beta = 2$, for $|Q| = 0$ and 1, and in total. We see that only the total (unrestricted) correlation matches a cosh function very well.

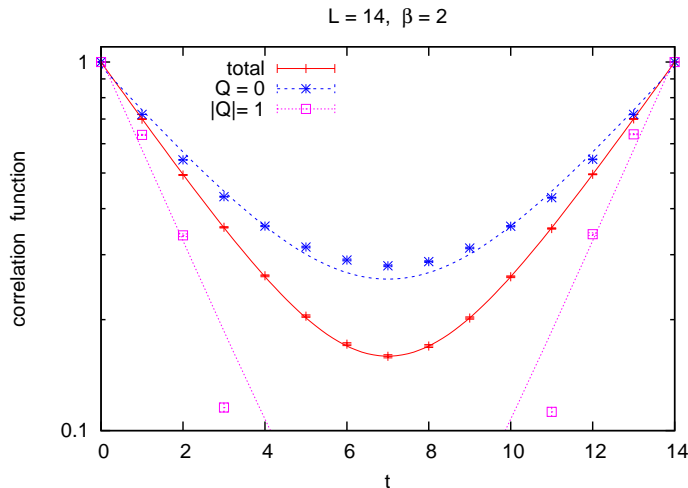


Figure 3. The correlation function for the 1d $O(2)$ model with $L = 14$, $\beta = 2$ for the sectors $|Q| = 0$ and 1, and in total. Only the complete correlation follows well a fit to a cosh function.

Now we increase the inverse coupling to $\beta = 4$, and we consider larger sizes in the range $L = 150 \dots 400$. Once we have evaluated $\xi_{|Q|}$ as well as possible, we use ξ_0 as an input for the summation formula (5.1) to obtain approximations $\xi_{1,\text{approx}}$ and $\xi_{2,\text{approx}}$, which are then compared to the directly measured values. Figure 4 shows good agreement over a broad range of L both for the standard action and for the Manton action. In particular for the smaller sizes L , this observation is highly non-trivial since there is a considerable splitting between the lengths $\xi_{|Q|}$. Of course, in very large volumes all values coincide, so this agreement becomes trivial.

Now we address the true correlation length ξ , which describes the decay of the correlation function measured over all topological sectors. Generally, in very large volumes all restricted values also coincide with the complete result, as eq. (5.1) shows, hence also this agreement becomes trivial. However, such large volumes are often inaccessible in Monte Carlo simulations. Therefore we explore whether in somewhat smaller volumes the correction terms on the right-hand-side of eq. (5.1) can help to still extract the correct result. The volume should not be too small, however, otherwise additional corrections, which are missing in approximation (5.1), become significant.⁴

⁴ An extension to higher-order corrections is discussed in Ref. [16].

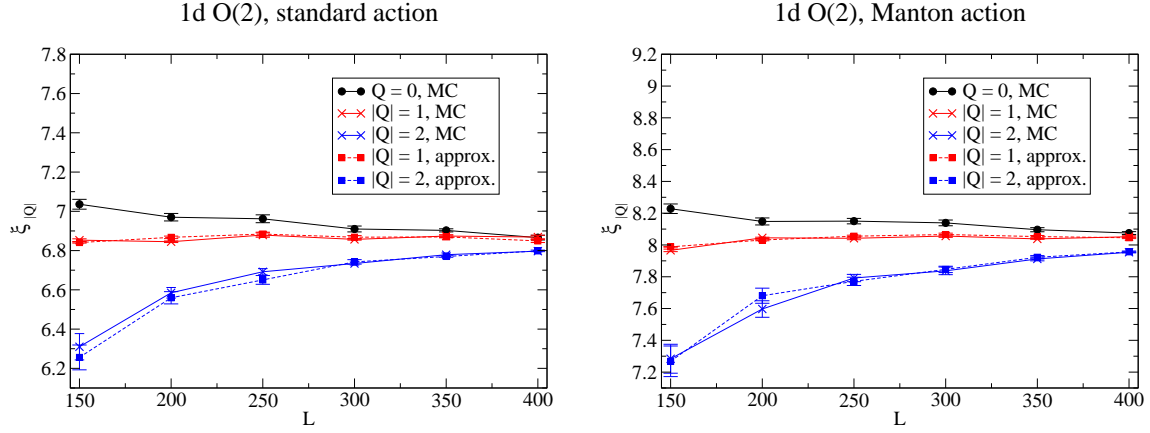


Figure 4. The topologically restricted correlation lengths ξ_0 , ξ_1 , ξ_2 measured directly in Monte Carlo (MC) simulations of the 1d $O(2)$ model at $\beta = 4$. For ξ_1 and ξ_2 these results are compared to the values obtained from the approximation formula (5.1), if ξ_0 is used as an input. We observe good agreement in all cases.

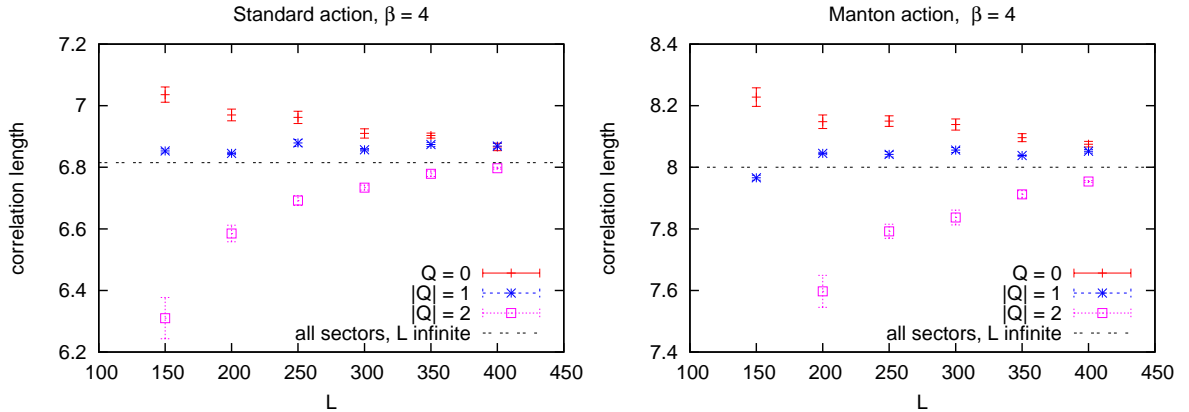


Figure 5. The analytic value of the correlation length ξ in the 1d $O(2)$ model (dashed lines), and numerical measurements for the topologically restricted correlation lengths ξ_0 , ξ_1 , ξ_2 in sizes $L = 150 \dots 400$. We see a clear splitting both for the standard action (on the left) and for the Manton action (on the right). Hence it is non-trivial that these measured values provide good estimate for ξ , when we insert them into approximation (5.1) and perform a least square fit for the three unknown terms. Corresponding results are given in Table 1.

Figure 5 shows the exact correlation length at $\beta = 4$, which is known analytically [11] (dashed lines), along with the numerically measured values for ξ_0 , ξ_1 , ξ_2 in sizes $L = 150 \dots 400$. Table 1 gives the results based on eq. (5.1), if we insert the numerical and the topologically restricted values in some range of sizes L . This is the procedure to handle a situation where the complete result is not known. Now the three unknown parameters are strongly over-determined, and we perform a least-square fit to obtain the estimates in Table 1. The fact that there are only small fitting errors confirms the consistency of this approach. Moreover, the resulting values are close to the exact values, which is again non-trivial regarding the significant splitting of ξ_0 , ξ_1 and ξ_2 (see Figure 5).

fitting range for L	Standard action			Manton action		
	250 – 400	300 – 400	theory	250 – 400	300 – 400	theory
ξ	6.77(5)	6.79(2)	6.815	7.95(5)	7.88(6)	8.000

Table 1. Fitting results for the correlation length ξ in the 1d $O(2)$ model at $\beta = 4$, based on the formula (5.1). We insert the numerically measured values for ξ_0, ξ_1, ξ_2 in some range for the size L , and determine the optimal approximation for ξ by a least-square fit. We arrive at results which are close to the theoretical value.

Finally we add an application of formula (5.1) to the 2d $O(3)$ model. Here our observable is the action density, *i.e.* the mean value of the action divided by the volume, $\langle S \rangle / V$. Figure 6 shows results for the sectors $|Q| = 0, 1, 2$ and for all configurations, in $L \times L$ volumes with $L = 8 \dots 32$. We see that they all converge to the same value for increasing size L .

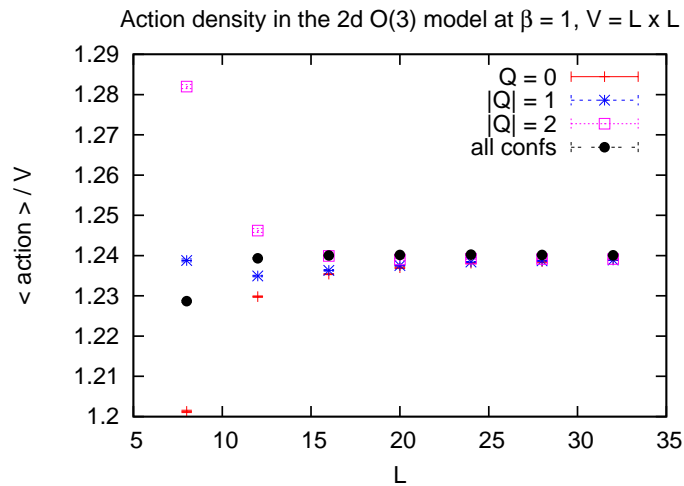


Figure 6. Numerical results for the action density of the 2d $O(3)$ model with the standard action at $\beta = 1$ in various $L \times L$ volumes. We show the complete result, as well as the values restricted to $|Q| = 0, 1$ or 2 .

If we were not able to measure the result over all configurations reliably — *i.e.* if we only had Monte Carlo histories that hardly ever change the topological sector — we could now use the restricted measurements in some range of L , insert them into formula (5.1) and estimate $\langle S \rangle / V$, as well as χ_t , with a least-square fit. Such results are displayed in Table 2. We see that

fitting range for L	16 – 24	16 – 28	16 – 32	directly measured in all sectors at $L = 32$
$\langle S \rangle / V$	1.24038(12)	1.24027(8)	1.24015(5)	1.24008(5)
χ_t	0.0173(6)	0.0169(5)	0.0164(5)	0.01721(4)

Table 2. Estimates for the action density $\langle S \rangle / V$ and for the topological susceptibility χ_t in the 2d $O(3)$ model at $\beta = 1$, based on topologically restricted results in some range of L . We find good agreement with the directly measured values, without topological restriction (last column).

even the use of modest volumes provides estimates, which agree well with the results of a direct complete measurement (this is feasible in this case thanks to the cluster algorithm).

6. Summary

Most Monte Carlo simulations of lattice field theory still have to be performed with local update algorithms. For theories with topological sectors, this often implies that the Monte Carlo history is confined to one sector over an enormous number of update steps — a problem, which is getting worse for decreasing lattice spacing. This concerns in particular QCD simulations with dynamical quarks.

In this case, it may happen that observables can be measured well only within a fixed sector, *i.e.* one is limited to topologically restricted expectation values $\langle \mathcal{O} \rangle_Q$. On the conceptual side, this rises algorithmic questions related to ergodicity. If we trust the restricted measurements $\langle \mathcal{O} \rangle_Q$, the next issue is to extract physical information from them.

An approximate formula derived in Ref. [14] allows in principle to obtain an estimate for the physical value $\langle \mathcal{O} \rangle$, based on restricted results in various topological sectors and in various volumes. Moreover, if the Monte Carlo history rarely changes Q , a direct measurement of the topological susceptibility χ_t is hardly possible. A fit to the formula (5.1) of Ref. [14] provides in addition an estimate for χ_t . That specific quantity can also be estimated from the correlation of the topological charge density, even within just one sector, based on another approximation formula put forward in Ref. [6], eq. (4.1).

Here we have tested both formulae in non-linear σ -models with topological sectors. In this case, we have the full-fledged result (involving all topological sectors) available for comparison, either analytically or numerically, hence we could check how far the approximations work. In Section 4 we tested eq. (4.1) to determine χ_t , and in Section 5 eq. (5.1) for the determination of full expectation values $\langle \mathcal{O} \rangle$ and χ_t .

Our results show that these formulae do work well in a suitable regime, where the assumptions for their derivations are decently satisfied. In particular, we need $\langle Q^2 \rangle \gtrsim 1.5$, and we should only involve sectors with $|Q| \leq 2$. These properties will be further explored in σ -models and in Yang-Mills gauge theory [9], in order to probe the prospects for applications in full QCD.

Acknowledgments

We thank Christopher Czaban, Arthur Dromard, Ivan Hip and Marc Wagner for helpful communication and collaboration. This work was supported by the Mexican *Consejo Nacional de Ciencia y Tecnología* (CONACyT) through project 155905/10 “Física de Partículas por medio de Simulaciones Numéricas”, as well as DGAPA-UNAM. The simulations were performed on the cluster of the Instituto de Ciencias Nucleares, UNAM.

- [1] Hasenfratz P, Laliena V and Niedermayer F 1998 *Phys. Lett. B* **427** 125
- [2] Berg B and Lüscher M 1981 *Nucl. Phys. B* **190** 412
- [3] Duane S, Kennedy A D, Pendleton B J and Roweth D 1987 *Phys. Lett.* **195** B 216
- [4] Fukaya H *et al* 2007 *Phys. Rev. Lett.* **98** 172001
- [5] Lüscher M 2010 *JHEP* **1008** 071
- [6] Aoki S, Fukaya H, Hashimoto S and Onogi T 2007 *Phys. Rev. D* **76** 054508
- [7] Aoki S *et al* 2008 *Phys. Lett. B* **665** 294
- [8] Fukaya H and Onogi T 2004 *Phys. Rev. D* **70** 054508
- [9] Bautista I, Bietenholz W, Czaban C, Dromard A, Gerber U, Hofmann C P, Mejía-Díaz H, Prado L and Wagner M, in preparation
- [10] Manton N 1980 *Phys. Lett. B* **96** 328
- [11] Bietenholz W, Brower R, Chandrasekharan S and Wiese U-J 1997 *Phys. Lett. B* **407** 283
- [12] Boyer T, Bietenholz W and Wuilloud J 2007 *Int. J. Mod. Phys. C* **18** 1497
- [13] Wolff U 1989 *Phys. Rev. Lett.* **62** 361
- [14] Brower R, Chandrasekharan S, Negele J W and Wiese U-J 2003 *Phys. Lett. B* **560** 64
- [15] Bietenholz W and Hip I 2008 *PoS LATTICE2008* 079; 2012 *J. Phys. Conf. Ser.* **378** 012041
Bietenholz W, Hip I, Shcheredin S and Volkholz J 2012 *Eur. Phys. J. C* **72** 1938
- [16] Dromard A and Wagner M, arXiv:1309.2483 [hep-lat]
- [17] Czaban C and Wagner M, arXiv:1310.5258 [hep-lat]